# Electronic Supplementary Information (ESI)

## Facile synthesis of spinel $CuCo_2O_4$ nanocrystal as a high-performance cathode catalyst for rechargeable Li-air batteries

Ying Liu [a], Lu-Jie Cao [b], Chen-Wei Cao [a], Man Wang [a], Kwan-Lan Leung [a], Shan-Shan Zeng [a], T. F. Hung [a], C. Y. Chung [a*], Zhou-Guang Lu [b*]

[a] Department of Physics and Materials Science, City University of Hong Kong, Hong Kong SAR, PR China

[b] Department of Materials Science & Engineering, South University of Science and Technology of China, Shenzhen, PR China

[*] *E-mail: appchung@cityu.edu.hk (CYC) ; luzg@sustc.edu.cn (LZG)*

### Experimental Section

**Synthesis of $CuCo_2O_4$ nanoparticles.** Spinel $CuCo_2O_4$ was synthesized using urea combustion method. Typically, 2 mmol $Cu(NO_3)_2{\cdot}3H_2O$ and 4 mmol $Co(NO_3)_2{\cdot}3H_2O$ were firstly dissolved in 80 ml distilled water. After dissolved completely, the obtained solution was stirred in 50 °C for 1 h. Then, 12 mmol urea was added to the solution and temperature was heated to 70 °C and maintained at this temperature for 24 h to slowly evaporate the water. The obtained powder was quickly ground to avoid absorbing water in air and then calcined at 400 °C for 6 h with a heating rate of 2 °C $min^{-1}$.

**Synthesis of $Co_3O_4$ nanoparticles.** The $Co_3O_4$ nanoparticles were synthesized by using a simple hydrothermal method. All reagents were of analytical grade and were used without further purification. In a typical procedure, 6 mmol $Co(NO_3)_2{\cdot}3H_2O$ was dissolved in deionized (DI) water (60 mL). The pH value was adjusted to 9 using concentrated sodium hydroxide solution

under vigorous stirring. Then the solution was transferred into a Teflon-lined stainless-steel autoclave and kept at 160 °C for 24 h. After the autoclave was cooled to ambient temperature, the sample was washed with DI water, vacuum dried and then thermally treated at 400 °C for 3 h.

**Material characterization.** The phases of the samples were characterized by a Siemens X-ray generator with a Cu Kα radiation (λ = 1.5405 Å). The scanning electron microscopy (SEM) was operated at a Joel JSM-820 field emission scanning electron microscope (Hitachi, Japan). Transmission electron microscopy (TEM) and high resolution transmission electron microscopy (HRTEM) were obtained on a Hitachi H-800 transmission electron microscope and a JEOL JEM-2100F TEM/STEM operated at 200 kV, respectively. Raman scattering was performed on Renishaw 2000 Raman microscope with 633 nm argon ion laser.

**Cell assembly.** The $CuCo_2O_4$ nanoparticles were used as cathodes for Li-air batteries assembled in coin cell (CR2025). The $O_2$ catalytic electrodes were prepared by a homogeneous ink, containing 30% $CuCo_2O_4$, 60% KB, and 10% PVDF onto a carbon paper disk (TGP-H-060). The total mass loading of the $CuCo_2O_4$/KB catalyst was approximately $0.6 \pm 0.05$ mg $cm^{-2}$. The sheet was heated at 80 °C for 12 h under vacuum to remove any residual solvent. In a glove box filled with pure argon, the batteries were assembled by using a lithium foil as anode, a Whatman glass fiber separator and TEGDME (1 M) + LiTFSI as electrolyte. Before testing, the batteries were placed into a closed glass box which was flushed with an 80% Ar and 20% $O_2$ for 3 h.

**Electrochemical measurement.** The Li-air batteries were discharged and charged at a galvanostatic current density of 50 mA $g^{-1}$ on an Arbin discharging/charging system between 2.2 and 4.2 V (vs. $Li^+$/Li). The specific capacity of $CuCo_2O_4$/KB nanoparticles were calculated based on the total mass of carbon on the electrode. The cycling performance of Li-air batteries was

analyzed by continuous discharge and charge with a limiting capacity of 1000 mAh $g^{-1}$ at 100 mA $g^{-1}$ and 400 mA/g. All electrochemical measurements were carried out at room temperature. To determine the composition of the discharged and charged products, the products were disassembled from coin cells, washed with dried dimethoxyethane, and dried in a glove box. Cyclic voltammetry (CV) was carried out between 2.0 and 4.7 V using a BioLogic VMP3 electrochemical station.

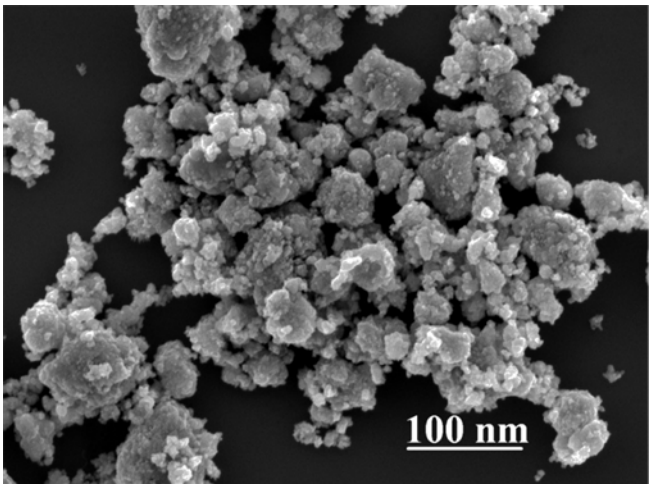


**Fig. S1** The SEM image of $CuCo_2O_4$ nanoparticles synthesized by urea combustion method.

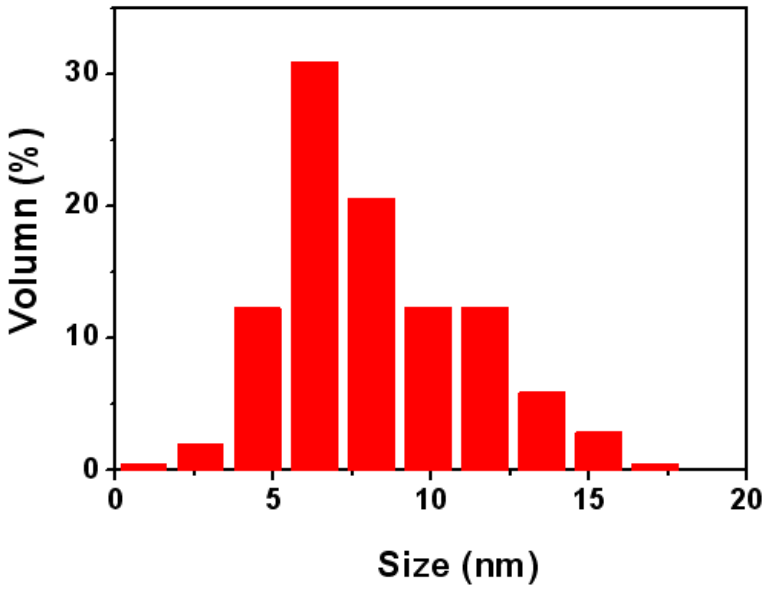


**Fig. S2** The size distribution of $CuCo_2O_4$ nanoparticles synthesized by urea combustion method.

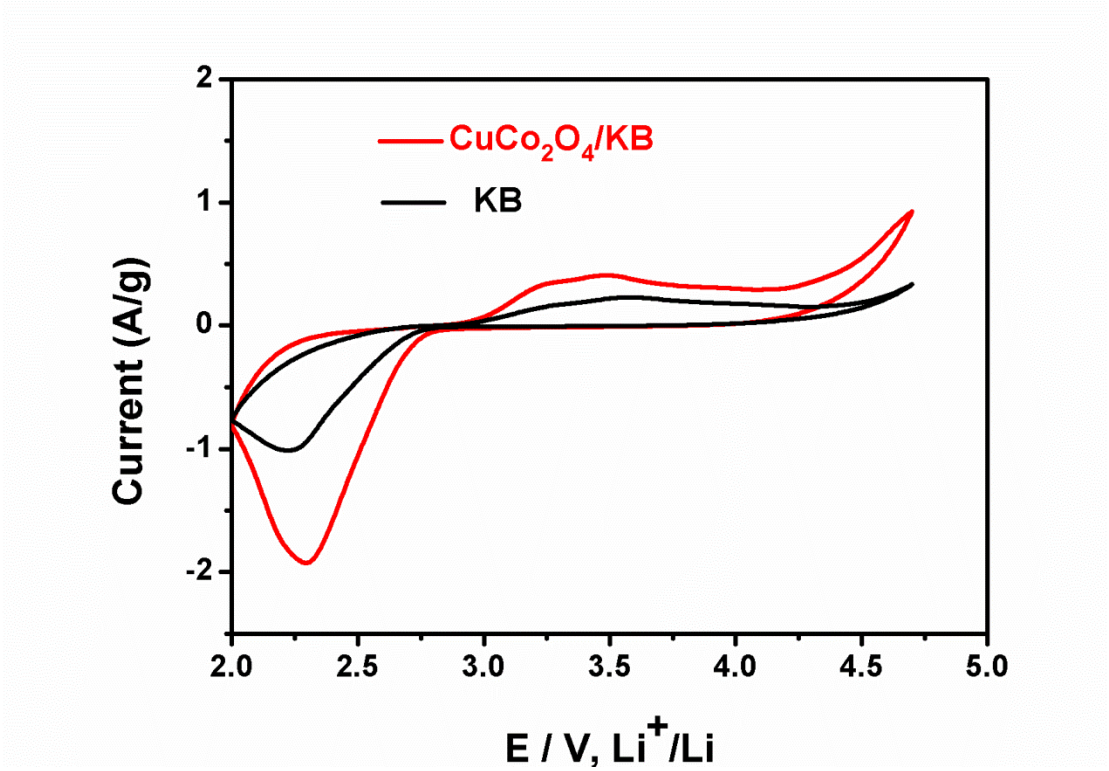


**Fig. S3** CV curves of $CuCo_2O_4$/KB and KB carbon-only electrode at a scan rate of 0.1 mV $s^{-1}$.

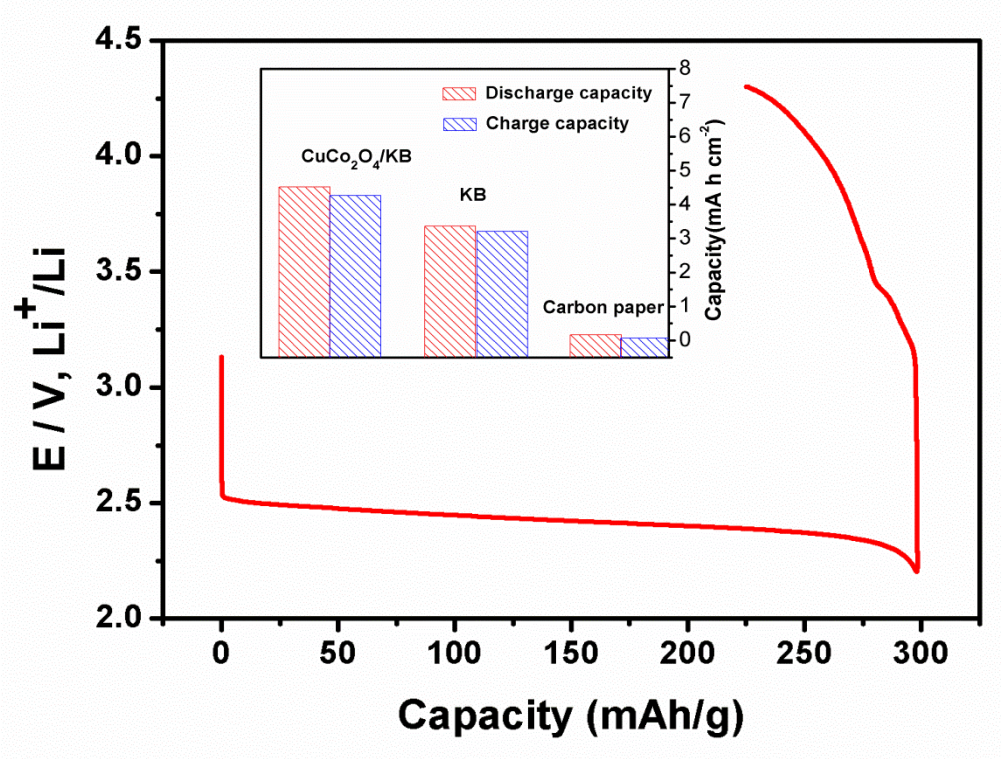


**Fig. S4** Discharge/charge profiles of the Li-air batteries without catalysts on the carbon paper at a current density of 50 mA $g^{-1}$ in the 1st cycle.

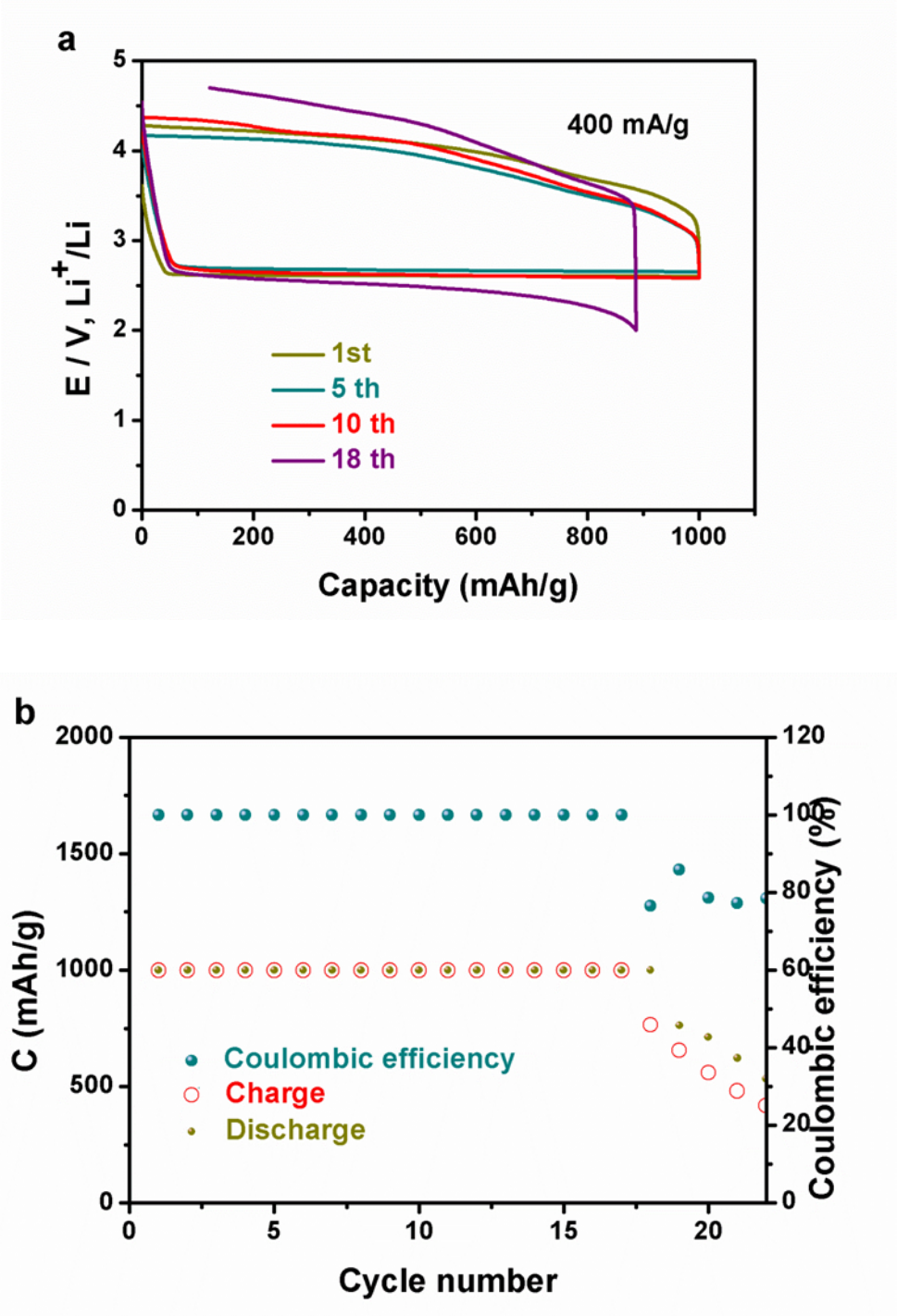


**Fig. S5** Discharge/charge profiles of the Li-air batteries with $Co_3O_4$ cathode over 22 cycles with a cut-off capacity of 1000 mAh $g^{-1}$, at 400 mA $g^{-1}$ (a) and their corresponding cycling performance and coulombic efficiency (b).

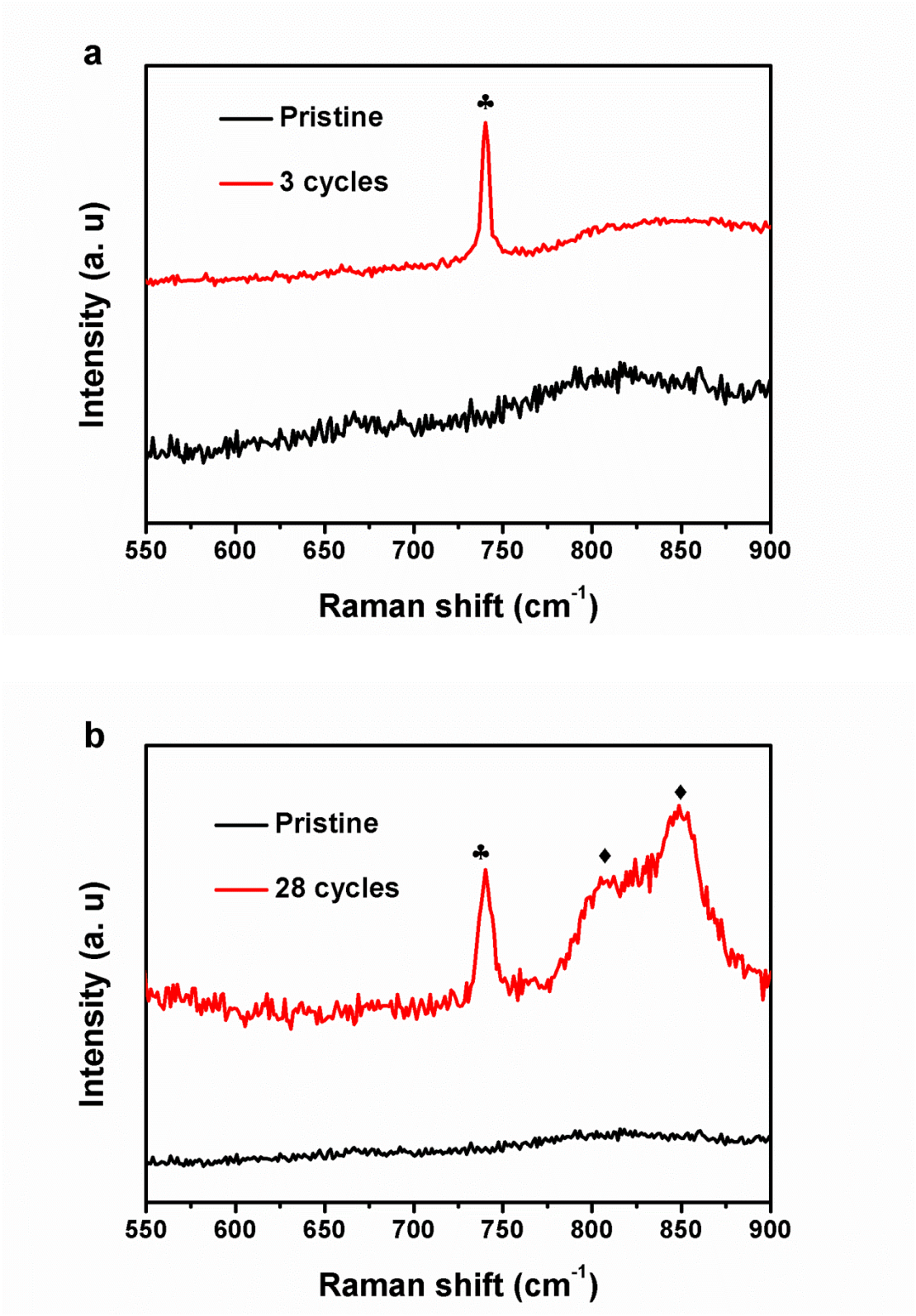


**Fig. S6** Raman spectra of $CuCo_2O_4$/KB electrode after 3 (a) and 28 cycles (b). The electrodes were collected and characterized after being fully charged. The signals of LiTFSI and $Li_2O_2$ are marked by ♣ and ♦, respectively.

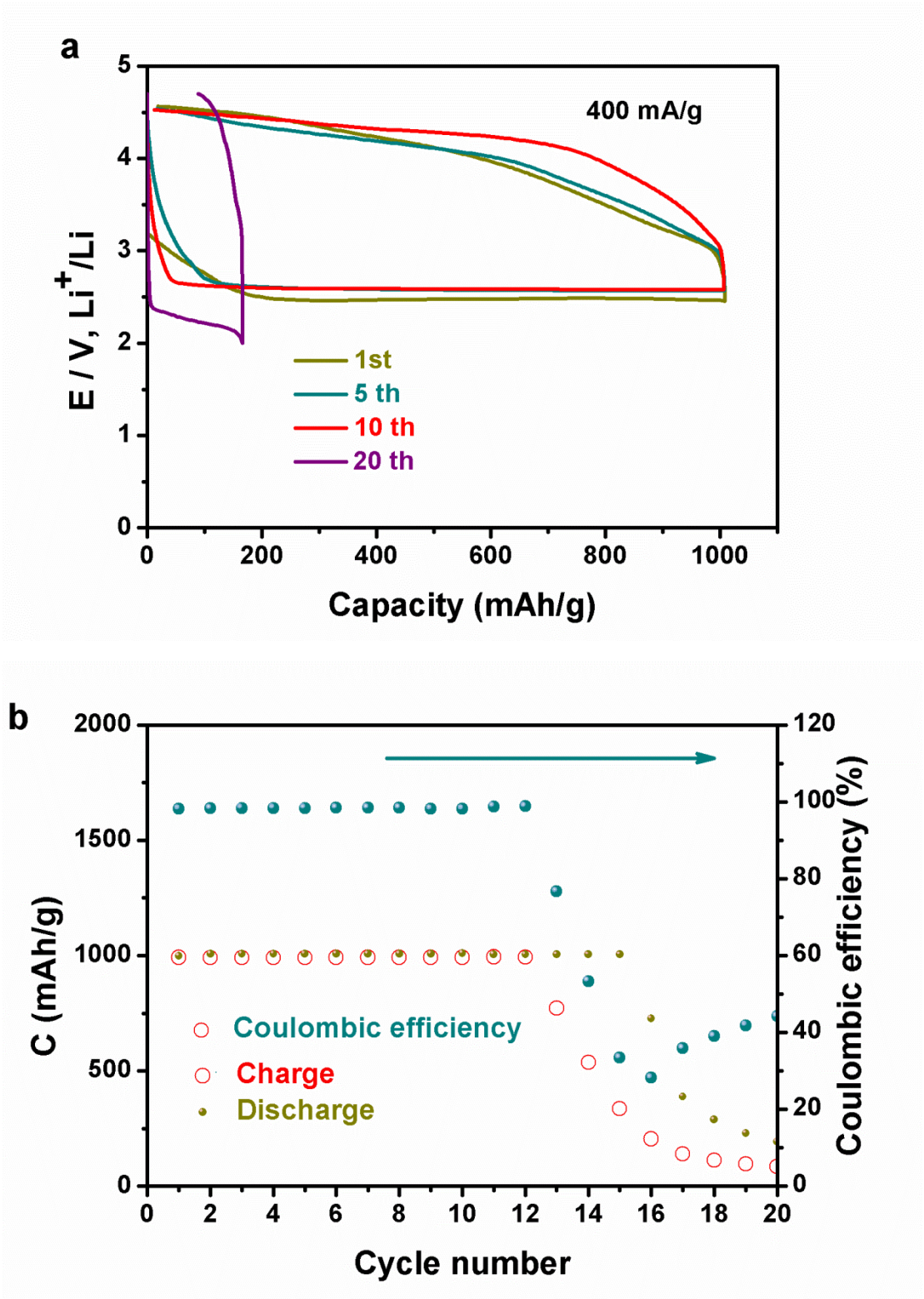


**Fig. S7** Discharge/charge profiles of the Li-air batteries with KB cathode over 20 cycles with a cut-off capacity of 1000 mAh $g^{-1}$, at 400 mA $g^{-1}$ (a) and the corresponding cycling performance and coulombic efficiency (b).

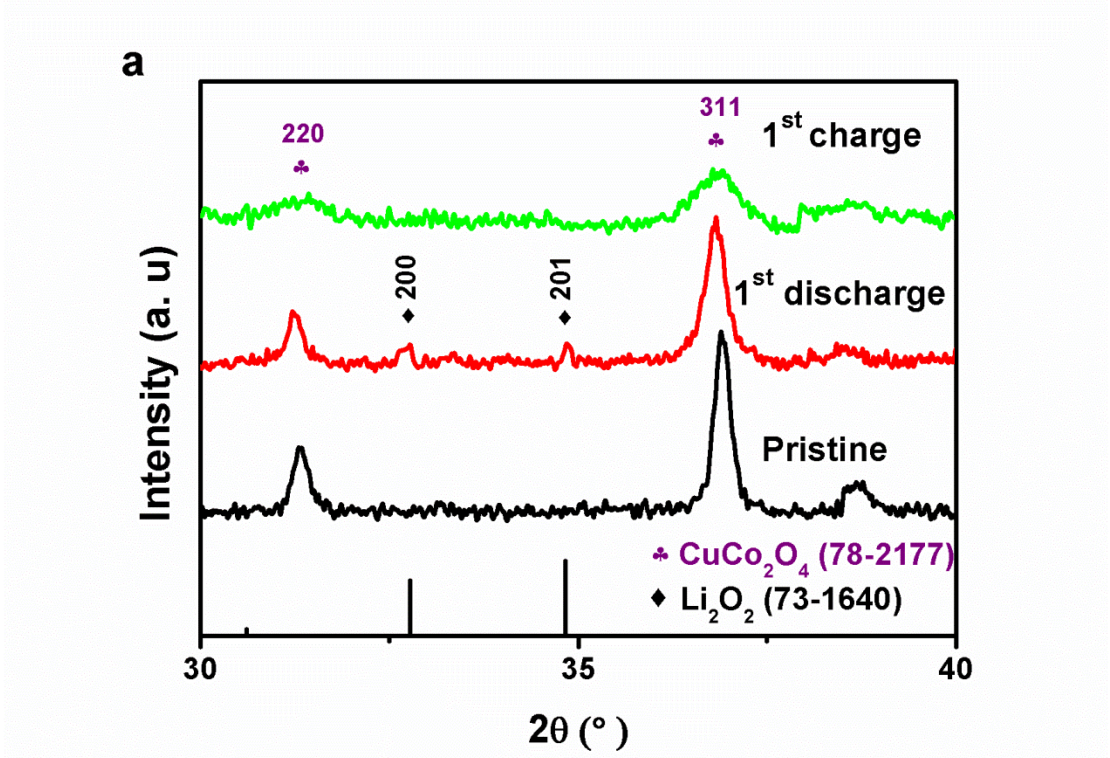
a
220
311
1st charge
200
201
1st discharge
Pristine
CuCo2O4 (78-2177)
Li2O2 (73-1640)
Intensity (a. u)
30
35
40
2θ (° )

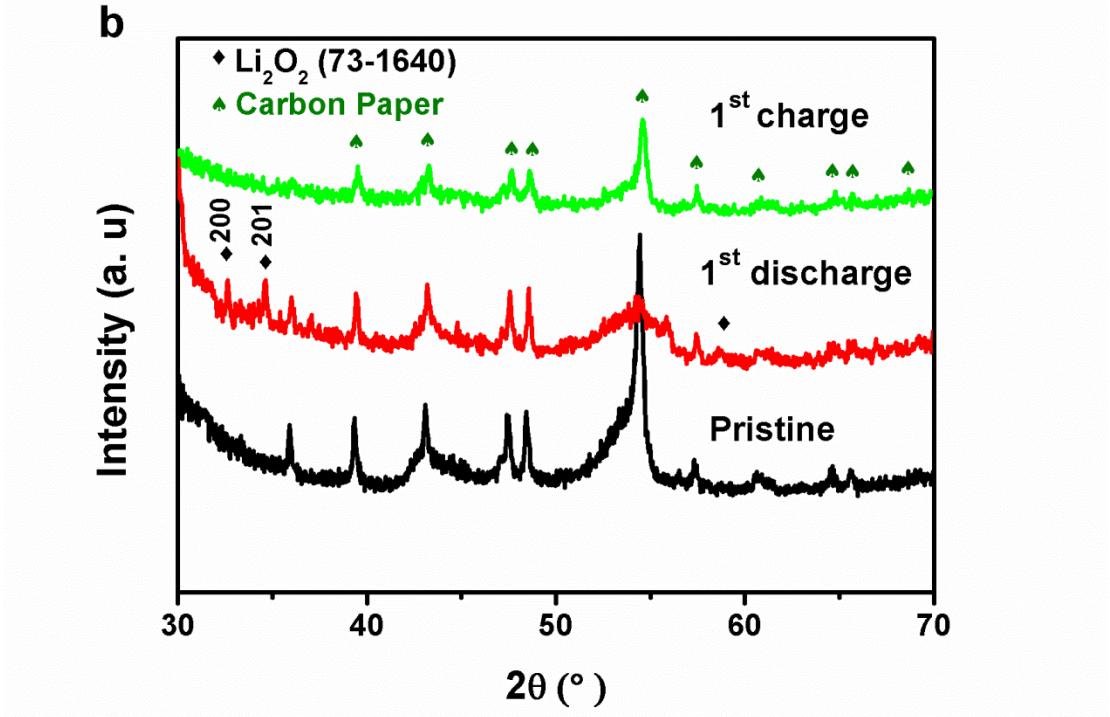
b
Li2O2 (73-1640)
Carbon Paper
1st charge
200
201
1st discharge
Pristine
Intensity (a. u)
30
40
50
60
70
2θ (° )

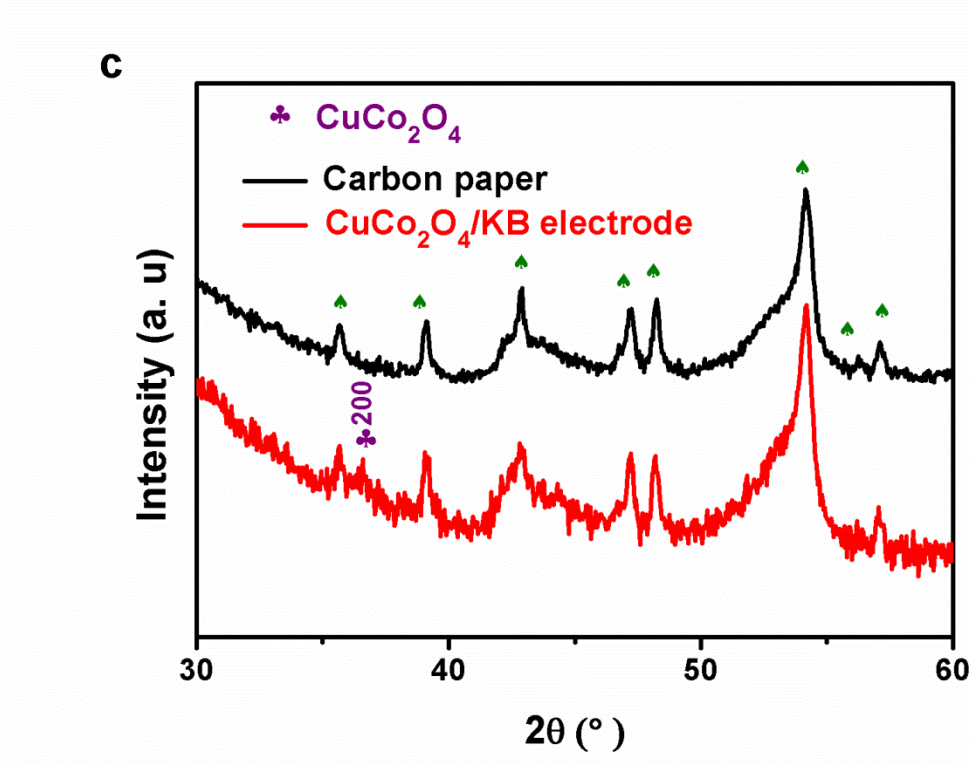


200

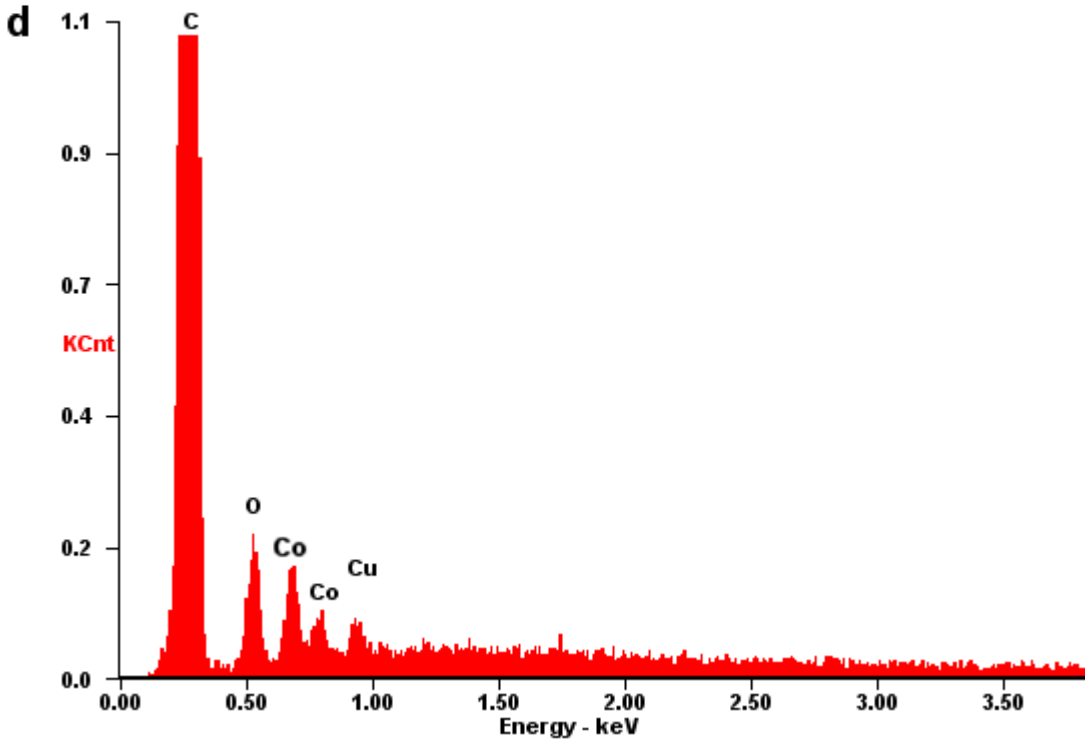


**Fig. S8** (a) The magnified XRD patterns of the pristine $CuCo_2O_4$/KB cathode (black), and after being fully discharged (red) and fully charged (green) of the 1st-cycle. The samples were collected after being scratched from the carbon paper. (b) XRD patterns of the KB coated on the carbon paper before (black) and after being fully discharged (red) and fully charged (green) of the 1st-cycle. (c) $CuCo_2O_4$/KB electrode on the carbon paper. (d) EDX of $CuCo_2O_4$/KB electrode.

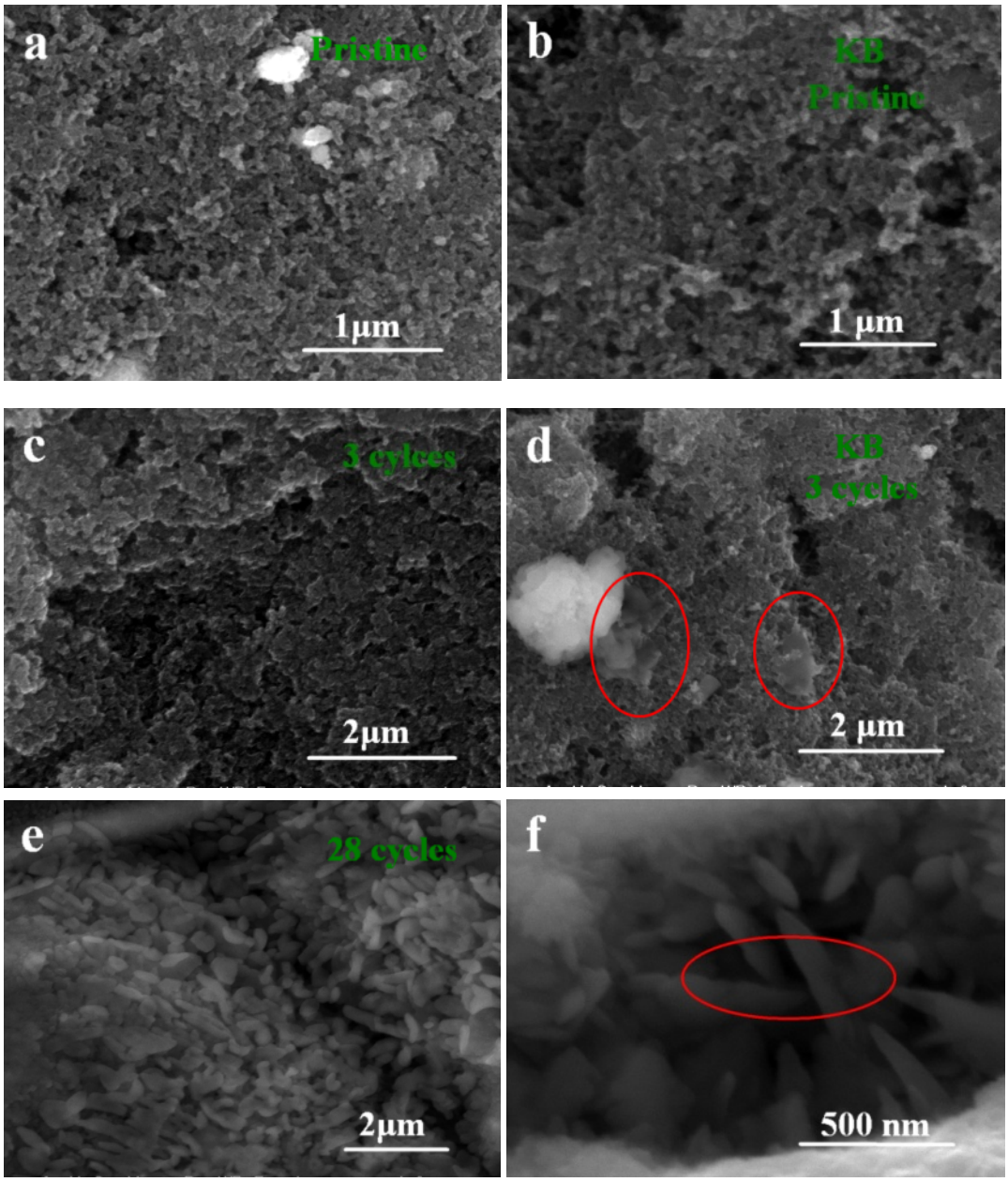


**Fig. S9** SEM images of $CuCo_2O_4$/KB based cathode and KB electrode. (a) pristine $CuCo_2O_4$/KB electrode, (b) pristine KB, (c) $CuCo_2O_4$/KB after 3 cycles, (d) KB electrode after 3 cycles,, (e) and (f) $CuCo_2O_4$/KB after 28 cycles.

**Tab. S1** A summary for the electrocheical performance of Li-oxygen/air batteries using $CuCo_2O_4$, $MnO_2$, and Co-based metal oxides reported as catalysts.

| Material | Morphology | Discharge potential (V) | ΔV* (V) | Cycle performance | Testing environment | Ref. |
|---|---|---|---|---|---|---|
| $CuCo_2O_4$ | Nanoparticles | ~2.72 | ~1.20 | 1000/50 cycles 100 mA/g | Mixed gas | This work |
| | | ~2.65 | ~ 1.35 | 1000/28 cycles 400 mA/g | | |
| $Co_3O_4$ | Nanosheets | ~2.75 | ~1.10 | 500/16 cycles 100 mA/g | $O_2$ | S1 |
| $Co_3O_4$ | Flakes | ~2.50 | ~1.00 | 1000/35 cycles 200 mA/g | $O_2$ | S2 |
| $Co_3O_4$ | Nanoparticles | ~2.60 | ~1.40 | 1000/30 cycles 200 mA/g | $O_2$ | 29 |
| | Nanofibers | ~2.69 | ~1.41 | 1000/80 cycles 200 mA/g | | |
| CNT-$Co_3O_4$ | Nanoparticles | ~2.70 | ~1.40 | ~700/3$^{th}$cycles 0.2 mA cm$^{-2}$ | $O_2$ | S3 |
| $MnO_2$ | Nanorods | ~2.62 | ~1.38 | 500/ 56 cycles 100 mA/g | $O_2$ | S4 |
| $NiCo_2O_4$ | Nanosheets | ~2.70 | ~1.30 | 500/50 cycles 200 mA/g | $O_2$ | S5 |
| $ZnCo_2O_4$ | Nanoflakes | ~2.60 | ~1.40 | 500/30 cycles 0.1 mA cm$^{-2}$ | $O_2$ | S6 |
| $MnCo_2O_4$ | Microsphere | ~2.70 | ~1. 40 | 1000/50 cycles 250 mA/g | $O_2$ | S7 |
| $Co_3O_4$-CuO | Microsphere | ~3.00 | ~1.20 | 250/20 cycles 0.2 mA cm$^{-2}$ | air | S8 |

* ΔV is the difference between discharge potential and charge potential at right-side current density.

## Supplementary References


S1 A. Riaz, K. N. Jung, W. Y. Chang, S. B. Lee, T. H. Lim, S. J. Park, R. H. Song, S. Yoon, K. H. Shin and J. W. Lee, *Chem. Commun.*, 2013, **49**, 5984.

S2 G. Y. Zhao, Z. M. Xu and K. N. Sun, *J. Mater. Chem. A,* 2013, **1**, 12862.

S3 T. H. Yoon, and Y. J. Park, *Nanoscale Res. Lett*., 2012, **7**, 1.

S4 Y. Qin, J. Lu, P. Du, Z. H. Chen, Y. Ren, T. P. Wu, J. T. Miller, J. G. Wen, D. J. Miller, Z. C. Zhang, and K. Amine, *Energy Environ. Sci.,* 2013, **6**, 519.

S5 B. Sun, X. D. Huang, S. Q. Chen, Y. F. Zhao, J. Q. Zhang, P. Munroec and G. X. Wang *J. Mater. Chem. A*, 2014, DOI: 10.1039/C4TA01888E.

S6 T. F. Hung, S. G. Mohamed, C. C. Shen, Y. Q. Tsai, W. S. Chang and R. S. Liu, *Nanoscale*, 2013, **5**, 12115.

S7 S. C. Ma, L. Q. Sun, L. N. Cong, X. G. Gao, C. Yao, X. G., L. H. Tai, P. Mei, Y. P. Zeng, H. M. Xie, and R. S. Wang, *J. Phys. Chem. C*, 2013, **117**, 25890.

S8 W. Yang, J. Salim, C. Ma, Z. H. Ma, C. W. Sun, J. Q. Li, L. Q. Chen, Y. Kim, *Electrochem., Commun.,* 2013, **28**, 13.